Calculation of the Geometry of the Water Molecule in Liquid Water

Thomas M. Nymand*,† and Per-Olof Åstrand‡

Department of Chemistry, Aarhus University, DK-8000 Århus C, Denmark, and Chemistry Laboratory III, H. C. Ørsted Institute, University of Copenhagen, DK-2100 København Ø, Denmark

Received: May 22, 1997; In Final Form: September 10, 1997[⊗]

The temperature dependence of the geometry of the water molecule in liquid water is calculated as a perturbation of its gas-phase geometry. The perturbation is assumed to depend only on the electrostatic and van der Waals interactions with the surrounding molecules. The geometry shift is thus given by the electric fields, their gradients, and the fluctuation potential obtained as ensemble averages in molecular dynamics simulations and quantum chemical calculations of field and field-gradient derivatives of the geometrical gradient and Hessian of the water molecule. The presented gas-to-liquid shifts ($\Delta r_{OH} \approx 1$ pm and $\Delta\alpha \approx 2°$) are of the same accuracy as both experiment and other theoretical investigations.

I. Introduction

Water is in many aspects a unique liquid. It is the most abundant liquid on earth, the most common solvent in chemistry, and it is essential in biochemistry.[1−3] Furthermore, liquid water has some anomalous properties such as having a high dielectric constant, a minimum of the specific heat capacity, C_p, at 30 °C, a density maximum at 4 °C, and a negative volume of melting.[2,4] It has been suggested that the special properties of liquid water is due to a true singularity of liquid water at −46 °C, which is just below the attainable supercooling temperature at −42 °C.[5,6] It is therefore not surprising that liquid water has been investigated extensively both experimentally and theoretically. Nonetheless, the underlying molecular mechanisms that would explain the properties of the liquid are far from fully understood.

A property that should be important for liquid water is the geometry of the water molecule in the liquid phase. The equilibrium geometry in the gas phase is $r = 0.9572$ Å and $\alpha_e = 104.52°$[7] and the vibrationally averaged geometry in ice Ih is $r_{OH} = 1.005$ Å and α 109.5°,[8] but for liquid water the geometry is not as well established.[9−14] The most recent experiment gives the vibrationally averaged values $r_{OD} = 0.970 \pm 0.005$ Å and $\alpha = 106.06° \pm 1.8°$ for D_2O.[14] The geometry of the water molecule in liquid water has been investigated theoretically mostly not only by considering clusters[15−18] but also by a simulation of a quantum molecule in a classical liquid.[19]

It is interesting that many of the rigid water potentials for molecular dynamics (MD) simulations such as SPC,[20,21] MCY,[22] TIP4P,[23] and NEMO[24−26] all use the gas-phase geometry, although they all intend to model liquid water. Since several of the potentials are successful in modelling many properties of water, it is expected that the liquid-phase geometry is close to the gas-phase geometry. Furthermore, the flexibility of the water molecule may be important for the properties of liquid water. The temperature dependence of dynamic properties are often modelled with transition state theory, i.e., it is assumed that an energy barrier is crossed.[27] It is possible that the geometry at the transition state is not the same as the average geometry, which will affect the transition rate. For instance, large effects have been noted for the diffusion coefficient in an MD simulation with a flexible SPC potential.[28,29]

The gas-to-liquid change of a molecular property A is normally defined as

$$A_{solvation} = A_{liquid} - A_{gas} \tag{1}$$

The small differences between the gas-phase and liquid-phase geometries and the successful assumption of using the gas-phase geometry in simulation potentials indicate that the difference between the liquid-phase and gas-phase geometries may be treated as a perturbation of the gas-phase geometry. The electrostatic contribution to $A_{solvation}$, which is the most important term for polar liquids, may be expanded by adopting perturbation theory (which, for example, has been done for nuclear shieldings[30,31]) as

$$A_E = A'_\gamma E_\gamma + \frac{1}{2}A''_{\gamma,\delta}E_\delta E_\gamma + ... + A'_{\gamma\delta}E_{\gamma\delta} + \frac{1}{2}A''_{\gamma\delta,\epsilon\sigma}E_{\epsilon\sigma}E_{\gamma\delta} + ... \tag{2}$$

where E_γ and $E_{\gamma\delta}$ are components of the electric field and the electric field gradient, respectively, arising from the presence of the solvent; A'_γ and $A''_{\gamma,\delta}$ are derivatives of A with respect to the electric field; and $A'_{\gamma\delta}$ and $A''_{\gamma\delta,\epsilon\sigma}$ are derivatives with respect to the electric field gradient. The Einstein summation convention will be used from this equation and on. The expansion in eq 2 has previously been used by us to calculate the gas-to-liquid chemical shifts of water.[32,33] In this work, we calculate the water geometry in the liquid phase assuming that the perturbation altering the geometry only depends on electrostatic and van der Waals interactions. The electrostatic contribution to the molecular gradient and Hessian has been calculated according to the expansion in eq 2 as

$$g_{E,\alpha} = g'^k_{\alpha,\gamma}\langle E^k_\gamma\rangle + {}^1/_2 g''^k_{\alpha,\gamma,\delta}\langle E^k_\delta E^k_\gamma\rangle + g'^k_{\alpha,\gamma\delta}\langle E^k_{\gamma\delta}\rangle \tag{3}$$

and

$$H_{E,\alpha\beta} = H'^k_{\alpha\beta,\gamma}\langle E^k_\gamma\rangle + {}^1/_2 H''^k_{\alpha\beta,\gamma,\delta}\langle E^k_\delta E^k_\gamma\rangle + H'^k_{\alpha\beta,\gamma\delta}\langle E^k_{\gamma\delta}\rangle \tag{4}$$

where we have used statistical mechanical ensemble averages of the electric fields and field-gradients. We have here truncated the series in eq 2 after the three most important terms. The indices α and β refer to the normal coordinates, and we therefore allow the gradient and Hessian components to depend on the electric field and field-gradient at all three atoms, as indicated

† Aarhus University.
‡ University of Copenhagen.
⊗ Abstract published in *Advance ACS Abstracts,* December 1, 1997.

S1089-5639(97)01706-4 CCC: $14.00

by the atom index k on field and field-gradient components. We are thus employing a distributed representation of the gradient and Hessian and their field derivatives, which has previously proven to be an appropriate way to treat other molecular properties such as the charge distribution[34−36] and polarizabilities.[37−39]

Following our previous considerations regarding the van der Waals contribution to the chemical shift,[32] we obtain the dispersive contributions to the molecular gradient and Hessian as

$$g_{\omega,\alpha} = {}^1/_2 g''^{k}_{\alpha,\gamma,\delta} \langle E_0^2 \rangle^{k}_{\gamma\delta} \tag{5}$$

and

$$H_{\omega,\alpha\beta} = {}^1/_2 H''^{k}_{\alpha\beta,\gamma,\delta} \langle E_0^2 \rangle^{k}_{\gamma\delta} \tag{6}$$

In these equations the fluctuation potential acting on the kth atom is taken from the NEMO potential[24,32]

$$\langle E_0^2 \rangle^{k}_{\alpha\beta} = \sqrt{C} \frac{\bar{\omega}^{\mathrm{A}} \bar{\omega}^{\mathrm{B}}}{\bar{\omega}^{\mathrm{A}} + \bar{\omega}^{\mathrm{B}}} \sum_j \alpha^{j}_{\gamma\delta} T^{kj}_{\alpha\gamma} T^{kj}_{\beta\delta} \tag{7}$$

where $\alpha_{\alpha\beta}$ is a component of an atomic polarizability tensor,[37] $T^{kj}_{\alpha\beta}$ is a component of the so called interaction tensor $(\nabla_\alpha \nabla_\beta (1/R_{kj}))$, $\bar{\omega}^{\mathrm{A}}$ is an averaged ionization potential of molecule A, and C is a correction factor of 1.89 calibrated from the H_2-H_2 system.[40]

Knowing the Hessian of the unperturbed water molecule ($\mathbf{H}^0$) and taking the gradient to be zero at the unperturbed geometry (which is true for an optimized geometry), we can use the Newton−Raphson method to determine the new molecular geometry $\mathbf{x}$ as

$$\mathbf{x} = \mathbf{x}^0 - (\mathbf{H}^0 + \mathbf{H}_{\mathrm{sol}})^{-1} \mathbf{g}_{\mathrm{sol}} \tag{8}$$

in matrix notation, where $\mathbf{x}^0$ is the unperturbed optimized geometry, $\mathbf{g}_{\mathrm{sol}} = \mathbf{g}_E + \mathbf{g}_\omega$ and $\mathbf{H}_{\mathrm{sol}} = \mathbf{H}_E + \mathbf{H}_\omega$. To determine this new geometry, we need statistical mechanical ensemble averages of electric fields, field gradients, and the fluctuation potential. We must also determine the various derivatives of the molecular gradient and Hessian with respect to the electric field and its gradient. The required ensemble averages have previously been calculated by us[32,33] and the needed derivatives have been determined using a *point charge method* as in ref 33. The calculation of these derivatives will be described in the following section. We will present our results in section III and draw conclusions in section IV.

II. Calculation of Gradient and Hessian Derivatives

The first and second derivative with respect to the electric field and the first derivative with respect to the field gradient of the molecular gradient and Hessian have been calculated using a *point charge method* previously used by us to calculate the quadrupole shielding polarizabilities for water.[33] The method is based on quantum chemical calculations on water where the molecule interacts with a set of point charges. A component of the molecular Hessian in a water molecule interacting with charge set i is the sum of the Hessian of water in vacuum $H^0_{\alpha\beta}$ and a difference Hessian, i.e.,

$$H_{\alpha\beta,i} = H^0_{\alpha\beta} + \Delta H_{\alpha\beta,i} \tag{9}$$

where we expand the difference Hessian according to eq 2 as

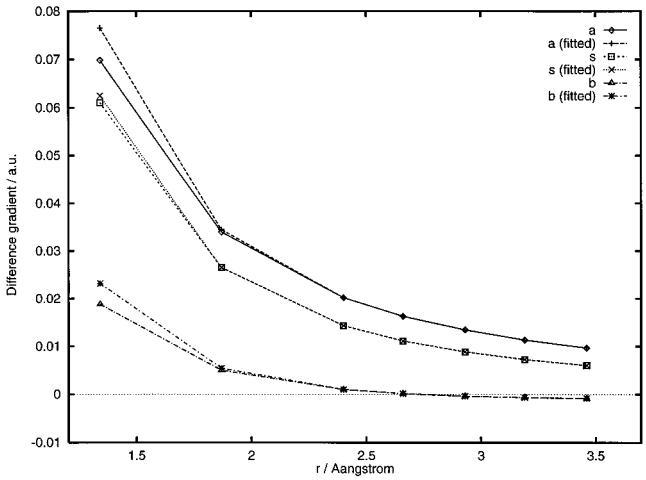

Figure 1. The molecular gradient in a water molecule interacting with a negative point charge of 1 au. The point charge is positioned at a distance r to the H atom at the line intersecting the H and O atoms. The letters a, s, and b refer to the asymmetric stretch, the symmetric stretch, and the bending components, respectively. The points at 1.34 and 1.87 Å were not included in the fit and thus demonstrate the ability to extrapolate the fit.

$$\Delta H_{\alpha\beta,i} = H'_{\alpha\beta,\gamma} E_{\gamma,i} + \frac{1}{2} H''_{\alpha\beta,\gamma,\delta} E_{\delta,i} E_{\gamma,i} + H'_{\alpha\beta,\gamma\delta} E_{\gamma\delta,i} \tag{10}$$

For clarity we have omitted the atom index. These equations also apply to the molecular gradient with the simplification that the gradient in vacuum (g^0_α) is zero, since we use a geometry optimized water molecule as our reference. For the gradient we thus get

$$\Delta g_{\alpha,i} = g'_{\alpha,\gamma} E_{\gamma,i} + {}^1/_2 g''_{\alpha,\gamma,\delta} E_{\delta,i} E_{\gamma,i} + g'_{\alpha,\gamma\delta} E_{\gamma\delta,i} \tag{11}$$

Herein lies the assumption, that the Coulombic interactions alone are responsible for the change in the molecular Hessian and gradient, i.e., possible penetration effects are not included. However, such effects were not found for the point-charge molecule distances adopted here, as is noted in Figure 1 for the H−X distance. We have carried out quantum chemical calculations at the SCF level and with a complete active space SCF (CASSCF)[41] wave function. In the CASSCF calculation, the 1s-electrons of oxygen have been kept inactive whereas we distribute the remaining electrons in $6A_1$, $3B_1$, $3B_2$, and $1A_2$ orbitals. We have used the DALTON program in all calculations.[42] The geometry optimizations have been carried out with a second order optimization routine.[43] The atomic natural orbital (ANO) basis sets by Widmark *et al.*[44] have been used in all calculations.

In Table 1 we present optimized geometries and harmonic vibrational frequencies for the isolated molecule for a number of contractions of the ANO basis set. Based on these results we decided to use the basis set in the [5s4p3d2*f*/4s3p2d] contraction at both correlation levels. We then performed both HF and CASSCF calculations of the molecular gradient and Hessian using this basis set yielding $H^i_{\alpha\beta}$ and g^i_α. In these calculations, the water molecule interacts with different partial charge distributions while held fixed at the optimal geometry. The parameters $H'_{\alpha\beta,\gamma}$, $H''_{\alpha\beta,\gamma,\delta}$, and $H'_{\alpha\beta,\gamma\delta}$ have been fitted to the set $\{\Delta H^i_{\alpha\beta}, E^i_\gamma, E^i_{\gamma\delta}\}$ using a least-squares method. The gradient parameters have been obtained in a similar manner. All three gradient and six Hessian fits have been done using a singular value decomposition (SVD) method,[45] since the parameters are not independent.

TABLE 1: Geometry and Harmonic Vibrational Frequencies for the Isolated Molecule

basis set	r_{OH}/Å	α/deg	ω_α/cm^{-1}	ω_s/cm^{-1}	ω_b/cm^{-1}
		HF			
ANO[3s2p1d/2s1p]	0.9483	106.41	4237.85	4124.21	1737.62
ANO[4s3p2d/3s2p]	0.9404	106.16	4234.50	4135.37	1760.36
ANO[4s3p2d1f/3s2p1d]	0.9403	106.36	4238.79	4137.37	1745.02
ANO[5s4p3d/4s3p]	0.9398	106.17	4227.10	4128.90	1761.69
ANO[5s4p3d2f/4s3p2d]	0.9397	106.31	4231.45	4132.09	1747.97
ANO[6s5p4d/5s4p]	0.9397	106.25	4224.44	4126.46	1762.78
ANO[6s5p4d3f/5s4p3d]	0.9397	106.32	4230.23	4130.23	1747.74
		CAS			
ANO[4s3p2d1f/3s2p1d]	0.9581	104.87	3981.80	3864.77	1654.44
ANO[5s4p3d2f/4s3p2d]	0.9580	104.79	3966.79	3851.32	1657.69
ANO[6s5p4d3f/5s4p3d]	0.9580	104.81	3965.33	3848.89	1657.37

TABLE 2: Electrostatic Effects on the Molecular Gradient in 10^{-3} au

		hydrogen				oxygen				
component	*T*/K	LF[a]	QF[b]	LFG[c]	D[d]	LF	QF	LFG	D	total
					HF					
g_s[e]	269	−14.5	1.12	5.12	−3.65	39.7	10.7	−1.68	22.1	58.9
	300	−13.5	0.891	4.41	−3.73	36.8	9.49	−1.72	21.2	53.8
	338	−12.5	0.667	3.73	−3.72	33.8	8.21	−1.67	19.9	48.4
	448	−9.94	0.250	2.30	−3.45	26.3	5.48	−1.34	16.4	36.0
g_b[f]	269	32.1	5.08	−0.858	13.8	−30.2	−4.22	2.02	−7.73	9.94
	300	29.4	4.42	−0.634	13.0	−28.0	−3.71	1.98	−7.44	8.95
	338	26.5	3.76	−0.449	12.1	−25.7	−3.20	1.87	−7.01	7.82
	448	19.9	2.40	−0.087	9.58	−20.1	−2.12	1.45	−5.77	5.25
					CAS					
g_s	269	−13.8	1.70	5.19	−2.59	32.5	11.3	−0.345	23.8	57.8
	300	−12.9	1.39	4.48	−2.75	30.2	10.0	−0.540	22.8	52.7
	338	−11.9	1.09	3.81	−2.82	27.7	8.66	−0.644	21.4	47.3
	448	−9.39	0.513	2.39	−2.76	21.6	5.79	−0.629	17.5	35.0
g_b	269	29.9	4.98	−0.787	14.0	−26.5	−4.10	1.84	−7.57	11.8
	300	27.4	4.33	−0.580	13.1	−24.5	−3.61	1.82	−7.28	10.6
	338	24.7	3.69	−0.410	12.2	−22.5	−3.11	1.73	−6.86	9.38
	448	18.4	2.35	−0.076	9.69	−17.6	−2.06	1.35	−5.64	6.49

[a] The linear field contribution. [b] The quadratic field contribution. [c] The linear field-gradient contribution. [d] The dispersion contribution. [e] The symmetric stretch component. [f] The bend component.

TABLE 3: Electrostatic Effects on the Molecular Hessian in 10^{-3} au for the HF Calculations

		hydrogen				oxygen				
component	*T*/K	LF[a]	QF[b]	LFG[c]	D[d]	LF	QF	LFG	D	total
H_{ss}	269	66.6	−5.60	−12.4	−2.37	−54.5	−13.6	11.0	−23.6	−34.5
	300	61.8	−4.79	−10.8	−1.83	−50.6	−12.0	10.2	−22.8	−30.8
	338	56.7	−3.98	−9.23	−1.35	−46.4	−10.3	9.22	−21.6	−27.0
	448	44.4	−2.33	−5.90	−0.43	−36.2	−6.80	6.73	−18.0	−18.4
H_{bb}	269	16.0	−2.83	−6.41	−5.84	−15.2	−2.96	8.37	−6.80	−15.7
	300	15.0	−2.46	−5.90	−5.48	−14.1	−2.62	7.63	−6.52	−14.5
	338	13.9	−2.10	−5.33	−5.05	−12.9	−2.27	6.83	−6.12	−13.1
	448	11.1	−1.34	−4.01	−3.99	−10.1	−1.53	4.92	−5.02	−9.01
H_{sb}	269	−33.9	−1.45	−5.83	−10.9	38.4	6.61	−11.6	13.0	−5.79
	300	−31.7	−1.21	−5.47	−10.3	35.6	5.83	−10.6	12.5	−5.33
	338	−29.3	−0.985	−5.02	−9.48	32.7	5.03	−9.52	11.8	−4.85
	448	−23.5	−0.565	−3.94	−7.46	25.5	3.35	−6.86	9.72	−3.75
H_{aa}	269	−34.5	−11.9	1.61	−28.7	16.5	4.83	14.1	1.62	−36.3
	300	−31.8	−10.3	1.41	−26.9	15.3	4.18	12.5	1.45	−34.1
	338	−28.9	−8.71	1.21	−24.8	14.0	3.53	12.2	1.27	−31.4
	448	−22.0	−5.49	0.791	−19.5	10.9	2.19	7.63	0.88	−24.6

[a] The linear field contribution. [b] The quadratic field contribution. [c] The linear field-gradient contribution. [d] The dispersion contribution.

III. Results

In our calculations, we have placed the water molecule in the *xz* plane with the oxygen atom at the origin and the hydrogen atoms at $(\pm x,0,z)$ and we will consider properties for the hydrogen atom situated at $(+x,0,z)$. With the sign we have chosen for the symmetric stretch coordinate q_s and the bend coordinate q_b, a step in the positive direction of q_s corresponds to a decreasing OH-bond distance and a positive step of q_b will correspond to a decreased bond angle.

In Table 2, we give the electrostatic effects on the nonvanishing terms of the molecular gradient at four different temperatures at both the HF and the CASSCF levels. The effects have been calculated using the temperature dependent electric fields and field gradients obtained by molecular dynamics simulation.[32,33] We present the contributions arising from the fields and field gradients at the hydrogen atoms and oxygen atom separately.

For the gradient, it is noted that all electrostatic contributions (LF, QF, and LFG) decrease in magnitude with increasing temperature. The temperature dependence of the dispersion contribution is smaller and, for the hydrogen contribution to the g_s component, nonuniform. We note that, when considering

TABLE 4: Electrostatic Effects on the Water Geometry

	T/K	r_{OH}/Å	Δr^a_{OH}/Å	α/deg	$\Delta\alpha^a$/Å
HF gas phase		0.9397		106.313	
HF	269	0.9514	0.0117	106.00	−0.31
LF	300	0.9505	0.0108	105.91	−0.40
	338	0.9495	0.0098	105.82	−0.49
	448	0.9472	0.0075	105.69	−0.62
HF	269	0.9571	0.0174	105.80	−0.52
LF + QF	300	0.9554	0.0157	105.72	−0.59
	338	0.9537	0.0140	105.65	−0.66
	448	0.9499	0.0102	105.56	−0.76
HF	269	0.9591	0.0194	106.22	−0.09
LF + QF + LFG	300	0.9571	0.0174	106.20	−0.11
	338	0.9550	0.0153	106.14	−0.17
	448	0.9505	0.0108	106.01	−0.30
HF	269	0.9694	0.0297	107.64	1.33
LF + QF + LFG + D	300	0.9667	0.0270	107.47	1.16
	338	0.9638	0.0241	107.26	0.95
	448	0.9574	0.0177	106.80	0.49
CAS gas phase		0.9580		104.79	
CAS	269	0.9782	0.0202	105.32	0.53
LF + QF + LFG	300	0.9760	0.0180	105.26	0.47
	338	0.9738	0.0158	105.15	0.36
	448	0.9690	0.0110	104.89	0.10
CAS	269	0.9915	0.0335	106.97	2.18
LF + QF + LFG + D	300	0.9884	0.0304	106.72	1.93
	338	0.9851	0.0271	106.44	1.65
	448	0.9777	0.0197	105.80	1.01

[a] Defined according to eq 1.

TABLE 5: Solvent Effects on the Molecular Gradient, Hessian, and Geometry at the HF and CAS Levels of Correlation

	HF values				CAS values			
property (T/K)	269	300	338	448	269	300	338	448
$g_s/10^{-3}$ au	58.9	53.8	48.4	36.0	57.8	52.7	47.3	35.0
$g_b/10^{-3}$ au	9.94	8.95	7.82	5.25	11.8	10.6	9.38	6.49
$H_{ss}/10^{-3}$ au	−34.5	−30.8	−27.0	−18.4	−21.1	−18.2	−15.2	−9.21
$H_{bb}/10^{-3}$ au	−15.7	−14.5	−13.1	−9.01	−15.7	−14.5	−13.0	−9.81
$H_{sb}/10^{-3}$ au	−5.79	−5.33	−4.85	−3.75	−6.09	−5.65	−5.19	−4.07
$H_{aa}/10^{-3}$ au	−36.3	−34.1	−31.4	−24.6	−27.0	−25.2	−23.1	−18.0
Δr_{OH}/pm	2.97	2.70	2.41	1.77	3.35	3.04	2.71	1.97
$\Delta\alpha$/deg.	1.33	1.16	0.95	0.49	2.18	1.93	1.65	1.01

TABLE 6: Solvent Effects on Vibrational Frequencies (in cm^{-1}) at the CAS Level

	G[a]			GS[b]			exptl[c]		
T/K	$\Delta\omega_a$[d]	$\Delta\omega_s$	$\Delta\omega_b$	$\Delta\omega_a$	$\Delta\omega_s$	$\Delta\omega_b$	$\Delta\omega_a$	$\Delta\omega_s$	$\Delta\omega_b$
269	−425	−441	42	−444	−467	−46	∼−310	∼−305	∼50
300	−387	−401	40	−405	−423	−41	∼−275	∼−265	∼45
338	−347	−359	37	−364	−376	−35	∼−245	∼−245	∼40
448	−256	−264	31	−271	−271	−23	∼−225	∼−230	∼35

[a] From the harmonic frequencies for the liquid geometry. [b] The solvation effect is added to the Hessian from G. [c] From ref 48. The temperatures used this in reference are 273, 323, 373, and 403 K. [d] $\Delta\omega = \omega_{liquid} - \omega_{gas}$.

the individual atomic contributions, we have a large linear field (LF) contribution, a much smaller quadratic field (QF) term and a linear field-gradient (LFG) contribution comparable in magnitude to that of the QF term. The dispersion (D) contribution is larger than both the QF and the LFG terms and has the same sign as the LF term. It thus contributes significantly to both gradient terms.

Considering the symmetric stretch component g_s, we note that the dominant term is the oxygen LF term. This term along with the oxygen QF and D terms tend to elongate the OH bond (due to our choice of sign for the corresponding coordinate q_s). This corresponds to the electrostatic attraction of oxygen towards the hydrogen atoms on neighboring molecules in the liquid. It is noted that the hydrogen LF term opposes this effect. We also note that LFG terms are rather small.

For the bending gradient component g_b, the picture is very different. The LF contributions from hydrogen and oxygen are of opposite sign and almost the same magnitude. The contributions from the QF and LFG terms and especially the D term thus become relatively important. When comparing the HF and the CAS results, we note that these are very similar, the most important difference being the slightly larger total CAS results for g_b. This difference arises mainly from the difference in the LF terms.

We also consider the electrostatic effects on the nonvanishing Hessian elements (Table 3) at the HF level. We note, that all contributions to the four terms decrease in magnitude with increasing temperature. Considering again the individual components, the picture is similar to the gradient results regarding the convergence of the electrostatic expansion. The LFG term is, however, slightly more important than the QF term. Again the D term is important, and due to the modest temperature dependence of this term, the influence of the D contribution becomes more important as the temperature is

increased. Furthermore, for the H_{ss} and H_{bb} components, we note that the hydrogen and oxygen dispersion contributions have the same sign. The overall contribution from the van der Waals interaction thus becomes more important than that of the electrostatic interactions for these components.

In Table 4, we give the liquid geometries and the normal coordinate displacements predicted by eq 8 for the four considered temperatures. We consider the effects from the different terms individually. We note that the LF effect is to elongate the OH-bond and to decrease the bond angle. The inclusion of the QF further increases the bond length substantially and decreases the bond angle to a smaller extent. The inclusion of the LFG effect, however, has a small impact on the bond length, whereas the bond angle is increased. When we include the effect arising from the van der Waals interaction, both the bond length and angle are substantially increased.

From the discussion in section I and the results of Table 1, it is noted that the geometry used in the NEMO simulation and the optimized Hartree−Fock (HF) geometry differ. We therefore have to examine what effect this difference might have on our results. In our previous work[32] it was noted, that the electric field on the hydrogen atom is directed along the OH-bond. We can thus test the importance of the effect arising from the geometry difference by rotating the electric field, field gradient, and fluctuation potential to correspond to a bond angle of 106.31° instead of the experimental gas-phase angle used in the simulation. We found that the effect on the bond elongation is very small and the effect on the resulting angle is less than 0.2° for all temperatures. A more proper way to study this effect would be to do the simulation with a flexible water geometry.

In Table 5, we present the total solvent effects on g, H, r_{OH}, and α. When comparing the calculated geometries, we note, that the CAS and HF numbers are similar for the OH-bond length, whereas the increase in bond angle is nearly twice as large for the CAS than for the HF calculation. A comparison with the experimental geometry ($r_{OH} = 0.970 \pm 0.005$ Å and $\alpha = 106.06 \pm 1.8°$)[7,14] shows that both calculations yield a much larger bond elongation than that established experimentally. It is, however, noted that the experimental gas-phase geometry is an equilibrium geometry,[7] whereas the experimental liquid-phase geometry is a vibrationally averaged geometry for the D_2O molecule.[14] The zero-point vibrational contributions for D_2O have been calculated to be $\Delta r_{OD} = 1.29$ pm and $\Delta\alpha = -0.019°$,[46] which for the bond distance is of the same size as the gas-to-liquid shift. Comparison with experimental bond distances is therefore difficult. It is furthermore noted that our gas-to-liquid shifts of the bond angle is in good agreement with experiment, $\Delta\alpha = 1.5 \pm 1.8°$.[7,14]

Effects on the molecular geometry from the intermolecular exchange repulsion has not been included even if they may be significant. Repulsive contributions would oppose the effects calculated here, which is interesting since we obtain rather small solvent effects on the molecular geometry.

Moriarty and Karlström have optimized the geometry of the water molecule at the Hartree−Fock level by studying a quantum molecule in a classical liquid.[19] Their bond distance elongation of 1.0 pm is in line with our values at the Hartree−Fock level (LF + QF + LFG) even if our value at room temperature is larger. The difference is, however, substantial for the bond angle. Moriarty and Karlström have obtained a value of $\Delta\alpha = 4.05°$ whereas we obtain small effects at the HF level. Our final values of about $\Delta\alpha = 2.0°$ is mainly a dispersive effect.

The gas-to-liquid shift of the intramolecular vibration frequencies origins from a shift of the molecular geometry (a perturbation of the molecular gradient) and external perturbations of the Hessian (the curvature of the potential is altered). A calculation of the harmonic frequencies for the liquid phase geometry is not trivial since we expand the potential around the gas-phase geometry. Such a calculation would therefore require fourth derivatives of the electronic energy with respect to the molecular geometry. We have, however, estimated the effect by carrying out a quantum chemical calculation of the harmonic frequencies for the isolated molecule at the liquid geometry to get the effects from altering the geometry and then added the solvent effects to the Hessian. The results are given in Table 6. The column designated G shows the changes in the vibrational frequencies arising from carrying out a quantum chemical calculation of the frequencies at the liquid geometry, and in the column GS the frequencies arising from adding $\mathbf{H}_{sol}$ to the liquid geometry Hessian is presented. The results are presented along with experimental data.[48]

When we examine the data in Table 6, we first of all note a reasonable agreement with experimentally determined vibrational shifts. We note that the stretching frequencies are more severely influenced by solvation than the bending frequency, which is confirmed experimentally. When comparing the columns G and GS, we note that the bending frequency is more influenced by the pure solvation than the stretching frequencies. We also note that the largest effect stems from altering the geometry of the water molecule. When we examine the temperature dependence of the vibrational shifts we should keep in mind that the vibrational shifts are determined experimentally at different temperatures than used in the calculations. We note that the temperature dependence is modeled qualitatively for the stretching modes, although the calculated temperature dependence seems to be slightly larger than that experimentally determined. Since we have the wrong sign for the bending frequency, we only model the temperature dependence of the magnitude of $\Delta\omega_b$.

IV. Discussion and Conclusions

In this work, we have calculated the geometry of the water molecule in liquid water with a perturbation approach. The results presented here are of similar accuracy as both other theoretical investigations and experimental data. Taking the simplicity of the model considered here into account, it is worthwhile exploring in more detail. It is especially advantageous that the quantum chemical and statistical mechanical computations have been separated into different parts.

It would be of interest to use this kind of approach for a flexible water potential. The model used here is possible to include in the NEMO potential[24,26] and should be feasible to employ directly in a simulation program. Even if the intramolecular motion is not classical, the zero-point vibrational contributions, which are the most important quantum effects, may be treated as discussed above with a mean-field approach.[47] It seems as zero-point vibrational contributions are important at least for the bond distance.[46]

Acknowledgment. Grants from the Danish Natural Research Council (SNF) are gratefully acknowledged.

References and Notes

(1) Eisenberg, D.; Kauzmann, W. *The Structure and Properties of Water*; Clarendon: Oxford, 1969.

(2) Franks, F., Ed. *Water: A Comprehensive Treatise*; Plenum Press: New York, 1972−81; Vol. 1−7.

(3) Horne, R. A. *Water and Aqueous Solutions: Structure, Thermodynamics and Transport Processes*; Wiley: New York, 1972.

(4) Stillinger, F. H. *Science* **1980**, *209*, 451−457.

(5) Speedy, R. J.; Angell, C. A. *J. Chem. Phys.* **1976**, *65*, 851−858.
(6) Angell, C. A. In *Water: A Comprehensive Treatise*; Franks, F., Ed.; Plenum Press: New York, 1977; Vol. 7.
(7) Benedict, W. S.; Gailar, N.; Plyler, E. K. *J. Chem. Phys.* **1965**, *24*, 1139.
(8) Kuhs, W. F.; Lehmann, M. S. *J. Phys. Chem.* **1983**, *87*, 4312.
(9) Narten, A. H.; Levy, H. A. *J. Chem. Phys.* **1971**, *55*, 2263.
(10) Walford, G.; Dore, J. C. *Mol. Phys.* **1977**, *34*, 21−32.
(11) Powles, J. G. *Mol. Phys.* **1981**, *42*, 757−765.
(12) Wu, A. Y.; Whalley, E.; Dolling, G. *Mol. Phys.* **1982**, *47*, 603−628.
(13) Gibson, I. P.; Dore, J. C. *Mol. Phys.* **1983**, *48*, 1019.
(14) Ichikawa, K.; Kameda, Y.; Yamaguchi, T.; Wakita, H.; Misawa, M. *Mol. Phys.* **1991**, *73*, 79−86.
(15) Xantheas, S. S.; Dunning, T. H., Jr. *J. Chem. Phys.* **1993**, *98*,-8037−8040.
(16) Xantheas, S. S.; Dunning, T. H., Jr. *J. Chem. Phys.* **1993**, *99*, 8774−8792.
(17) Schütz, M.; Bürgi, T.; Leutwyler, S.; Bürgi, H. B. *J. Chem. Phys.* **1993**, *99*, 8701−8711.
(18) Estrin, D. A.; Paglieri, L.; Corongiu, G.; Clementi, E. *J. Phys. Chem.* **1996**, *100*, 8701−8711.
(19) Moriarty, N. W.; Karlström, G. *J. Chem. Phys.* **1997**, *106*, 6470−6474.
(20) Berendsen, H. J. C.; Postma, J. P. M.; van Gunsteren, W. F.; Hermans, J. In *Intermolecular Forces*; Franks, F., Ed.; Reidel: Dordrecht, 1981; p 331.
(21) Berendsen, H. J. C.; Grigera, J. R.; Straatsma, T. P. *J. Phys. Chem.* **1987**, *91*, 6269−6271.
(22) Matsuoka, O.; Clementi, E.; Yoshimine, M. *J. Chem. Phys.* **1976**, *64*, 1351.
(23) Jorgensen, W. L. *J. Am. Chem. Soc.* **1981**, *103*, 335.
(24) Wallqvist, A.; Karlström, G. *Chem. Scr.* **1989**, *A29*, 131.
(25) Wallqvist, A.; Ahlström, P.; Karlström, G. *J. Phys. Chem.* **1990**, *94*, 1649−1656; *J. Phys. Chem.* **1991**, *95*, 4922 (erratum).
(26) Åstrand, P.-O.; Linse, P.; Karlström, G. *Chem. Phys.* **1995**, *191*, 195−202.
(27) Debye, P. *Polar Molecules*; Chemical Catalog: New York, 1929.
(28) Anderson, J.; Ullo, J. J.; Yip, S. *J. Chem. Phys.* **1987**, *87*, 1726−1732.
(29) Wallqvist, A.; Teleman, O. *Mol. Phys.* **1991**, *74*, 515−533.
(30) Buckingham, A. D. *Can. J. Chem.* **1960**, *38*, 300−307.
(31) Batchelor, J. G. *J. Am. Chem. Soc.* **1975**, *97*, 3410−3415.
(32) Nymand, T. M.; Åstrand, P.-O.; Mikkelsen, K. V. *J. Phys. Chem. B* **1997**, *101*, 4105−4110.
(33) Nymand, T. M.; Åstrand, P.-O. *J. Chem. Phys.* **1997**, *106*, 8332−8338.
(34) Port, G. N. J.; Pullman, A. *FEBS Lett.* **1973**, *31*, 70−74.
(35) Karlström, G. On the Evaluation of Intermolecular Potentials. In *Proceedings from 5th Seminar on Computational Methods in Quantum Chemistry*; Max-Planck-Institut für Physik und Astrophysik: Groningen, 1981.
(36) Stone, A. J. *Chem. Phys. Lett.* **1982**, *83*, 233.
(37) Karlström, G. *Theor. Chim. Acta* **1982**, *60*, 535.
(38) Stone, A. J. *Mol. Phys.* **1985**, *56*, 1065−1082.
(39) Ángyán, J. G.; Jansen, G.; Loos, M.; Hättig, C.; Hess, B. A. *Chem. Phys. Lett.* **1994**, *219*, 267−273.
(40) Karlström, G. *Theor. Chim. Acta* **1980**, *55*, 233−241.
(41) Roos, B. O. In *Ab Initio Methods in Quantum Chemistry*; Lawley, K. P., Ed.; Wiley: Chichester, 1987.
(42) Helgaker, T.; Jensen, H. J. Aa.; Jørgensen, P.; Olsen, J.; Ågren, H.; Andersen, T.; Bak, K. L.; Bakken, V.; Christiansen, O.; Dahle, P.; Dalskov, E. K.; Enevoldsen, T.; Fernandez, B.; Heiberg, H.; Hettema, H.; Jonsson, D.; Kirpekar, S.; Kobayashi, R.; Koch, H.; Mikkelsen, K. V.; Norman, P.; Packer, M. J.; Ruud, K.; Saue, T.; Taylor, P. R.; Vahtras, O. DALTON, an *ab initio* electronic structure program.
(43) Helgaker, T. U.; Almlöf, J.; Jensen, H. J. Aa.; Jørgensen, P. *J. Chem. Phys.* **1986**, *84*, 6266.
(44) Widmark, P.-O.; Malmqvist, P.-Å.; Roos, B. O. *Theor. Chim. Acta* **1990**, *77*, 291.
(45) Press, W. H.; Teukolsky, S. A.; Vetterling, W. T.; Flannery, B. P. *Numerical Recipes*; Cambridge University Press: Cambridge, 1992.
(46) Fowler, P. W.; Raynes, W. T. *Mol. Phys.* **1981**, *43*, 65−82.
(47) Åstrand, P.-O.; Mikkelsen, K. V. *J. Chem. Phys.* **1996**, *104*, 648−653.
(48) Ford, T. A.; Falk, Michael *Can. J. Chem.* **1968**, *46*, 3579−3586.